

Electron interactions in the $(\eta^2\text{-C}_{60})\text{Pd}[\text{P}(\text{Ph}_2)\text{C}_5\text{H}_4]_2\text{Fe}$ complex

L. G. Bulusheva,^{a*} A. V. Okotrub,^a V. V. Bashilov,^b and V. I. Sokolov^b

^aA. V. Nikolaev Institute of Inorganic Chemistry, Siberian Branch of the Russian Academy of Sciences,
3 prosp. Akad. Lavrent'eva, 630090 Novosibirsk, Russian Federation.

Fax: +7 (383) 330 9489. E-mail: bul@che.nsk.su

^bA. N. Nesmeyanov Institute of Organoelement Compounds, Russian Academy of Sciences,
28 ul. Vavilova, 119991 Moscow, Russian Federation.

Fax: +7 (495) 135 5085

The electronic structure of the $(\eta^2\text{-C}_{60})\text{Pd}[\text{P}(\text{Ph}_2)\text{C}_5\text{H}_4]_2\text{Fe}$ complex was calculated by the "hybrid" B3LYP method. Comparison of the experimental X-ray emission C-K α spectrum and theoretical spectrum of the compound demonstrated that the electron interactions between the C_{60} core, palladium atom, and organometallic fragment are described correctly in the framework of the quantum chemical method used. The electronic structure of the organometallic fullerene complex can be presented as a set of blocks of orbitals corresponding to different types of chemical bond.

Key words: fullerene C_{60} , metal complexes, electronic structure, quantum chemical calculations, B3LYP method, X-ray emission spectra.

The core structure of fullerenes induces strain of the carbon–carbon bonds, which results in activity of these molecules in different addition reactions.^{1,2} A molecule of the most stable fullerene C_{60} contains bonds of two types: a common bond combining the pentagon and hexagon ((5,6)-bond) and a shorter bond separating two hexagons ((6,6)-bond). The first of them can be considered as an ordinary bond, while the second bond behaves as a double bond. The surface of C_{60} can be presented as a system of conjugated double bonds. Therefore, the molecule manifests properties characteristic of unsaturated hydrocarbons. In particular, fullerenes, including C_{60} , form η^2 -complexes with transition metals.^{3,4}

Organometallic fullerene derivatives exhibit selective catalytic activity⁵ and unusual optical⁶ and electronic properties. The $(\eta^2\text{-C}_{60})\text{Pd}[\text{P}(\text{Ph}_2)\text{C}_5\text{H}_4]_2\text{Fe}$ complex is an example of a C_{60} bimetallic compound in which the palladium atom is directly bound to the carbon core and the iron atom enters in the composition of the bidentate diphosphine palladium-chelating ligand. Another specific feature of this complex is combining of fragments with different types of chemical bond. The electron density of the frontier orbitals of ferrocene is mainly localized on the metal atom, the highest occupied molecular orbital (HOMO) of triphenylphosphine represents virtually a lone electron pair of phosphorus, and the C_{60} molecule accumulates many π -electrons. It seems of interest for the chemistry of organometallic compounds to elucidate whether the electronic structures of the fragments retain individuality in the complex and to reveal orbitals in-

involved in electron interactions. The electrochemical study of $(\eta^2\text{-C}_{60})\text{Pd}[\text{P}(\text{Ph}_2)\text{C}_5\text{H}_4]_2\text{Fe}$ showed⁷ that the palladium atom is a charge transfer bridge from the ferrocene fragment to the core of C_{60} .

One of the methods that allows the direct investigation of the electronic structure of a substance is X-ray emission spectroscopy (XES). An X-ray emission spectrum appears due to the transition of valent electrons to the core levels with preliminarily created vacancies.⁸ Owing to the dipole selection rules and the localization of inner levels, this spectrum contains information on the local partial density of occupied states. These data can be compared to the results of quantum chemical calculation of the compound under study. This helps to interpret experimental data and serves as a criterion for applicability of the approximation used for compounds of the indicated type.

The purpose of the present work is to study electron interactions in the $(\eta^2\text{-C}_{60})\text{Pd}[\text{P}(\text{Ph}_2)\text{C}_5\text{H}_4]_2\text{Fe}$ complex by the XES and quantum chemistry methods.

Experimental

The $(\eta^2\text{-C}_{60})\text{Pd}[\text{P}(\text{Ph}_2)\text{C}_5\text{H}_4]_2\text{Fe}$ complex was synthesized according to an earlier described procedure.⁷

The X-ray emission C-K α spectra of fullerene C_{60} and the $(\eta^2\text{-C}_{60})\text{Pd}[\text{P}(\text{Ph}_2)\text{C}_5\text{H}_4]_2\text{Fe}$ complex were measured on a vacuum laboratory spectrometer. Samples were deposited on a copper support and cooled to the temperature of liquid nitrogen in a chamber of an X-ray tube with a copper anode (operating

conditions: $U = 6 \text{ kV}$, $I = 0.5 \text{ A}$). A single crystal of ammonium biphtalate (NH_4AP) was used as a crystal analyzer. The procedure of its use for C-K α spectra measuring has been described earlier.⁹ The resolution of the X-ray spectra was $\sim 0.4 \text{ eV}$, and the accuracy of determination of the energy of X-ray lines was $\pm 0.15 \text{ eV}$.

The quantum chemical calculation of the $(\eta^2\text{-C}_{60})\text{Pd}[\text{P}(\text{Ph}_2)\text{C}_5\text{H}_4]_2\text{Fe}$ complex was performed by the B3LYP method¹⁰ from the Jaguar program package.¹¹ The B3LYP method is "hybrid," because the Hartree–Fock method and a set of functionals are used in the calculation of electron interactions. A combination of different approximations makes it possible to decrease the error of determination of the metal–carbon bond length.¹² The polarized 6-31G** basis set was used for light elements (H, C), while a split basis set including AOs of the valent shell and the closest (to the latter) core shell served for atoms of heavy elements (P, Pd, Fe).

Using the NMR data⁷ on equivalence of the phosphorus atoms in the $(\eta^2\text{-C}_{60})\text{Pd}[\text{P}(\text{Ph}_2)\text{C}_5\text{H}_4]_2\text{Fe}$ complex, the molecule was constructed in such a way that the palladium atom was arranged above the center of the (6,6)-bond of the C_{60} core, and the Ph rings formed a "propeller" by analogy to the structure of triphenylphosphine PPh_3 . The geometry of the molecule was optimized in the C_s symmetry point group by the analytical method to a gradient value of $5 \cdot 10^{-5} \text{ au } \text{\AA}^{-1}$. The calculated bond lengths and bond angles were compared with the results of X-ray diffraction measurements of the $(\eta^2\text{-C}_{60})\text{Pd}(\text{PPh}_3)_2$ complex with a similar structure¹³ (values in parentheses): Pd–C, 2.10 \AA (2.08 \AA); Pd–P, 2.38 \AA (2.30 \AA); angle C–Pd–C 38.5° (40.2°); C–Pd–P 105.4° (109.7°). This comparison demonstrates that the interactions of the fullerene, palladium atom, and ligand were described correctly in the framework of the quantum chemical method used.

The results of quantum chemical calculations of the complex were taken into account for plotting the theoretical C-K α spectrum. The energy of the X-ray transition was assumed to be equal to the difference between the energies of the valent (i) and inner (j) levels

$$E_{ij} = \epsilon_i - \epsilon_j. \quad (1)$$

When calculating the intensity of the X-ray transition, we used an assumption that the X-ray transition occurs within the same A atom due to the localization of the 1s-AO of carbon. The line intensity was calculated by the formula

$$I_{ij} = \sum_A \sum_n \sum_m |C_{jm}^A C_{in}^A|^2, \quad (2)$$

where A designates the carbon atoms of the complex; C_{jm} and C_{in} are coefficients for the carbon 1s-AO and 2p-AO composing the j th and i th molecular orbitals (MOs) of the compound. The calculated intensities were normalized to the maximum value and broadened by the Lorentz lines with a half-width at half-height of 0.8 eV . The theoretical C-K α spectrum was coupled to the experimental spectrum by an increase in the calculated energies of transitions by 10 eV , which compensated an increase in the energy of the X-ray transition in the ionized state.

Partial densities of the occupied states of carbons in the C_{60} , C_6H_5 , and C_5H_4 fragments constituted the complex were calculated as sums of the C2p-AOs squared coefficients composing the valent MO. The density of the occupied states of phospho-

rus, palladium, and iron in the complex was constructed for the P3p-AO and valent s-AO and d-AO of metals. The energy scale corresponds to the Kohn–Sham energies for the occupied MOs, which can be interpreted as vertical ionization potentials of a molecule.¹⁴

The graphical representation of the structures of MOs of the complex was obtained using the Molden program package.¹⁵

Results and Discussion

The experimental X-ray emission C-K α spectra of fullerene C_{60} and the $(\eta^2\text{-C}_{60})\text{Pd}[\text{P}(\text{Ph}_2)\text{C}_5\text{H}_4]_2\text{Fe}$ complex are shown in Fig. 1, curves 1 and 2. Four main features A–D can be distinguished in the spectrum of fullerene (see Fig. 1, curve 1). High-energy maxima A and B at ~ 282.0 and 280.6 eV correspond to the π -system of C_{60} , and the most intense maximum D at $\sim 275.7 \text{ eV}$ corresponds to the σ -system. Maximum C at 278.2 eV is formed due to the X-ray transitions of σ - and π -electrons. The C-K α spectrum of C_{60} was interpreted in detail.^{9,16} The C-K α spectrum of the complex (see Fig. 1, curve 2) retains the main features of the spectrum of fullerene, because $\sim 70\%$ carbon in the composition of the complex

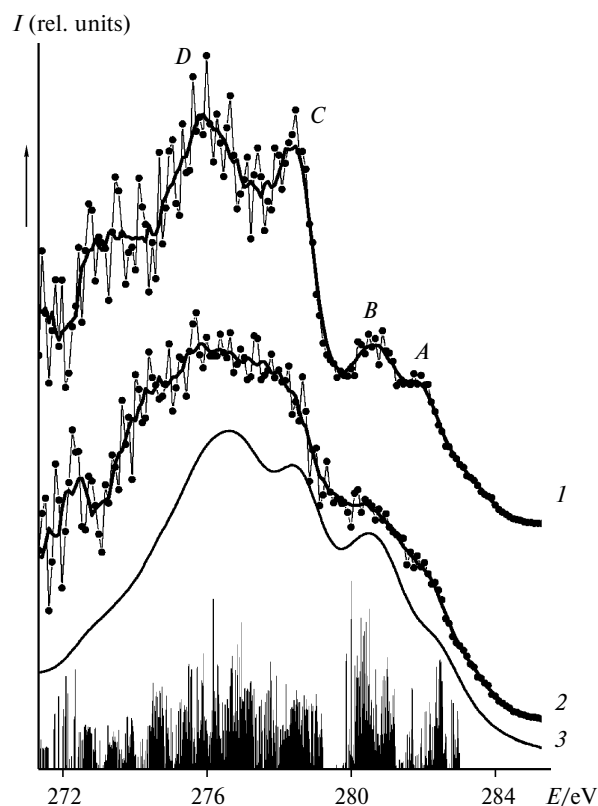


Fig. 1. Experimental X-ray emission C-K α spectra of fullerene C_{60} (1) and the $(\eta^2\text{-C}_{60})\text{Pd}[\text{P}(\text{Ph}_2)\text{C}_5\text{H}_4]_2\text{Fe}$ complex (2) and the B3LYP-calculated theoretical C-K α spectrum of this complex (3). Vertical lines characterize the relative intensity of X-ray transitions.

belong to the C_{60} core. The main differences between the spectra are the disappearance of the gap between maxima *C* and *D* and a decrease in the intensity of high-energy maximum *A* in the C-K α spectrum of the complex. The theoretical spectrum (see Fig. 1, curve 3) plotted by the results of calculation of the molecule is also characterized by four specific features. The distance between them and their relative intensities agree with the experimental values, which indicates that the quantum chemical approach used is appropriate for studies of electronic structures of organometallic fullerene complexes and that the interactions between the molecules in the solid state are weak.

These differences between the C-K α spectra of fullerene and the $(\eta^2-C_{60})Pd[P(Ph)_2C_5H_4]_2Fe$ complex can be related to (1) decrease in symmetry of C_{60} , (2) contribution of the electron density of the phenyl and cyclopentadienyl rings, and (3) appearance of additional MOs providing bonding of particular fragments in the complex. To reveal the MOs that provide interactions in the complex, we calculated the densities of the occupied states of carbon (in the fragments C_{60} , C_6H_5 , and C_5H_4), palladium, phosphorus, and iron (Fig. 2). For the C_{60}

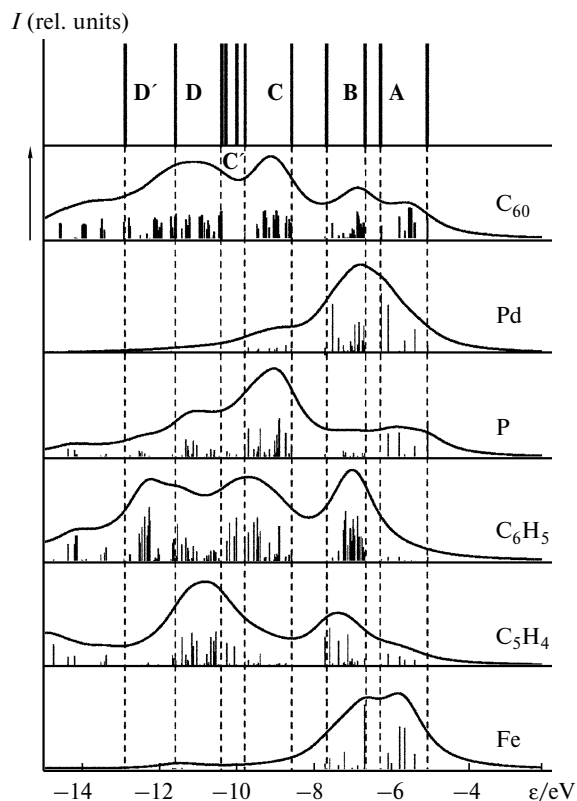


Fig. 2. Partial densities of the occupied states of carbon (in the C_{60} , C_6H_5 , and C_5H_4 fragments), palladium, phosphorus, and iron in the $(\eta^2-C_{60})Pd[P(Ph)_2C_5H_4]_2Fe$ complex and the energy positions of blocks of the molecular orbitals of the complex with different types of chemical bond. Vertical lines under the curves correspond to the MOs involving orbitals of atoms that compose a fragment.

fragments, the results of calculation agree with the shape of the C-K α spectrum of fullerene C_{60} (see Fig. 1, curve 1). The triple-humped structure characteristic of the density of states of carbon in the phenyl rings is similar to the C-K α spectrum of benzene,¹⁷ and the density of states of carbon in the Cp rings correspond to the data of photoelectron¹⁸ and X-ray fluorescence spectroscopies¹⁹ for ferrocene. This result shows that the carbon-containing fragments retain, in general, their individual character in the $(\eta^2-C_{60})Pd[P(Ph)_2C_5H_4]_2Fe$ complex. The metal atoms are mainly involved in the formation of the HOMO with the ionization potentials from 5 to 8 eV, while the 3p-AOs of phosphorus make the most noticeable contribution to the MOs with lower energies.

Analysis of the electronic structure of the complex shows that the density of occupied states can be presented as a set of six blocks of MOs corresponding to different types of electron interactions. The most characteristic MOs of each block are schematically shown in Fig. 3. Block A unifies the MOs of the complex that provide mainly the interaction between the π -system of fullerene and palladium, phosphorus, and iron atoms (see Fig. 2). The electron density of the Ph rings is not virtually involved in the formation of these MOs, and a small contribution of π -electrons of the Cp rings provides weak bonding with the d-AOs of iron and AOs of phosphorus. A specific feature of the MOs in block A is no localization of the electron density on any fragment. Figure 3, *a* presents the HOMO of the complex, which consists of the orbitals of C_{60} by ~72%, AOs of Pd by 13%, and a lone electron pair of phosphorus by 15%.

The electron density of the HOMO has the π -type distribution over the C_{60} core. However, the C—Pd—P bonding occurs through this orbital according to the σ -type. Orbitals of all structural fragments of the $(\eta^2-C_{60})Pd[P(Ph)_2C_5H_4]_2Fe$ complex are involved in the formation of MOs of block B. The density of states in the energy interval from -6.7 to -7.7 eV corresponds, to a great extent, to the π -systems of C_{60} , C_6H_5 , and C_5H_4 . Many MOs are characterized by electron density localization on any carbon-containing fragment. Other orbitals of block B provide bonding between the carbon and metal atoms. Figure 3, *b* presents the MO, which exemplifies electron interactions between the C_{60} , Pd, P, and C_6H_5 fragments and metal—ring bonding in the ferrocene fragment.

Block C is separated from block B by the gap with a width of ~1 eV, indicating basic differences in the character of chemical interactions provided by the MOs of these blocks. In the energy interval from -8.6 to -9.8 eV, the density of states of the complex is formed with a small participation of the AOs of palladium and involves no electrons of iron. The maximum contribution of 3p-electrons of the phosphorus atoms provides its bonding with the Ph rings and palladium atom. A great part of the

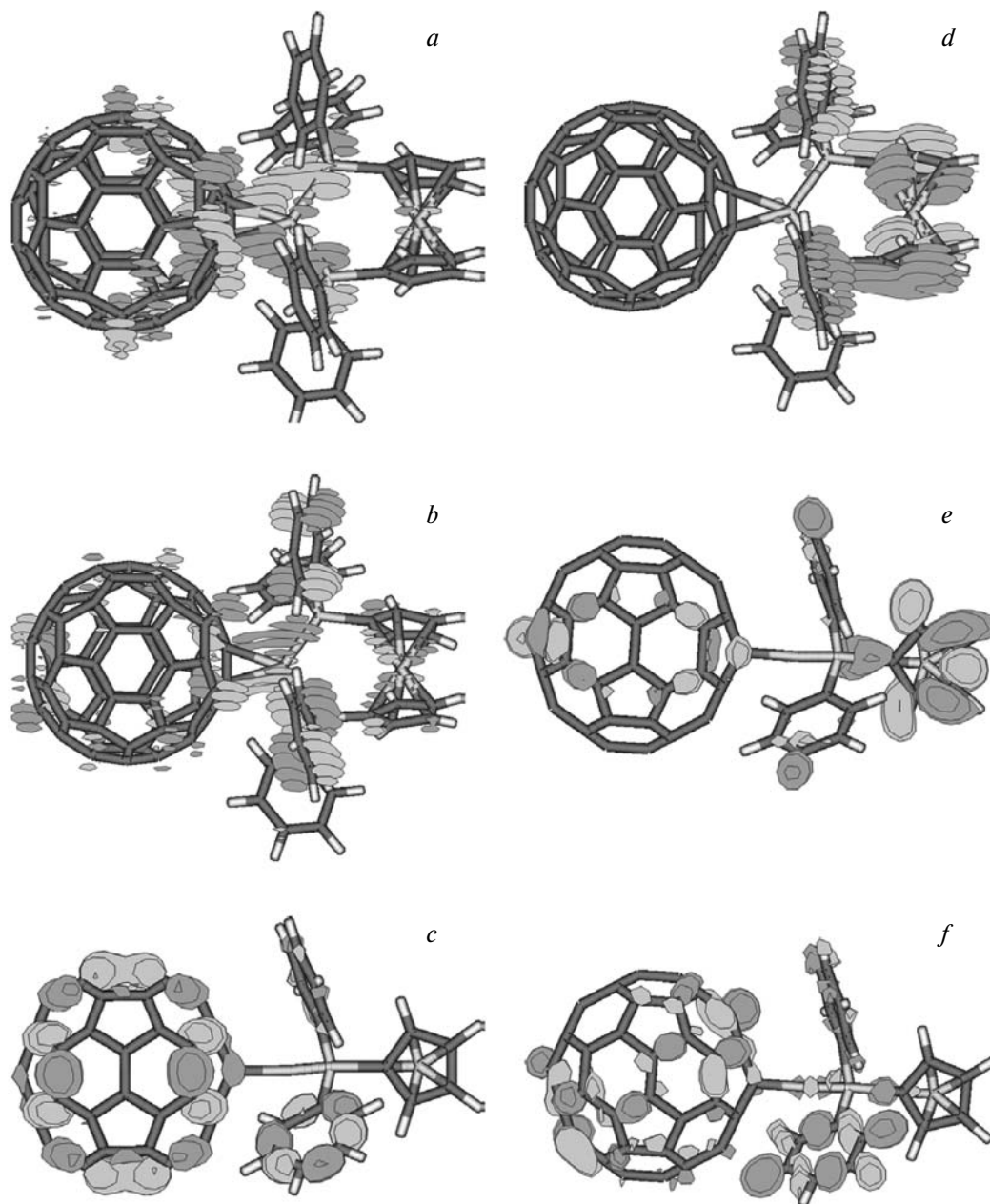


Fig. 3. Structure of the molecular orbitals of the $(\eta^2\text{-C}_{60})\text{Pd}[\text{P}(\text{Ph}_2)\text{C}_5\text{H}_4]_2\text{Fe}$ complex in blocks **A** (a), **B** (b), **C** (c), **C'** (d), **D** (e), and **D'** (f) shown in Fig. 2. The change in color corresponds to a change in the phase of the wave function.

electron density of the MOs in block **C** is formed by the σ -systems of the carbon-containing fragments and can be localized on one fragment or simultaneously on several fragments (see Fig. 3, c). Block **C'** occupies a narrow (~ 0.2 eV) energy interval and includes MOs corresponding to the π -systems of the Ph and Cp rings. A small contribution of the AOs of phosphorus provides bonding between these fragments (see Fig. 3, d). Block **D** includes the maximum number of MOs of the complex. The density of states of the block is mainly formed by the σ -systems

of C_{60} , C_6H_5 , and C_5H_4 . However, there are several MOs corresponding to deep bonding π -orbitals of fullerene and cyclopentadienyl ligands. Figure 3, e presents an example showing the σ -orbital of the complex formed by electrons of all carbon-containing fragments. In addition, this orbital provides bonding of the phosphorus atoms with the Cp fragments. The carbon—hydrogen interactions in the Ph and Cp rings also occur due to the MOs in block **D**. Orbitals composing block **D'** (see Fig. 3, f) resemble the MOs of the previous block. The main difference is the

absence of a noticeable contribution of the electron density of the ferrocene fragment to the formation of MOs in this block.

The presented analysis of the electronic structure of the $(\eta^2\text{-C}_{60})\text{Pd}[\text{P}(\text{Ph}_2)\text{C}_5\text{H}_4]_2\text{Fe}$ complex makes it possible to interpret the C-K α spectrum of the compound (see Fig. 1, curve 2). High-energy maximum *A* in the spectrum is formed due to the X-ray transitions of π -electrons of the C_{60} core (MOs of block **A**), whereas maximum *B* concerns the π -systems of all carbon-containing fragments (MOs of block **B**). These bands are broadened compared to those in the C-K α spectrum of fullerene (see Fig. 1, curve 1) due, most likely, to the appearance of additional MOs that provide the interaction of the carbon atoms with the phosphorus and metal atoms. The spectral features of *C* and *D* correspond mainly to the σ -system in the complex bonding the C—C, C—H, and C—P atoms. The appearance of an additional density between maxima *C* and *D* compared to the C-K α spectrum of fullerene C_{60} is caused by the contribution of π -electrons of the Ph and Cp fragments (block **C**).

Chemical bonding of fullerene C_{60} with the 1,1'-bis(diphenylphosphino)ferrocene ligand through the palladium atom involves the HOMO, which indicates that these interactions are weak. The charges calculated according to Mulliken for C_{60} , Pd, and Fe are equal to -0.35 , -0.29 , and -0.23 *e*, respectively. The high positive charge on the phosphorus atoms ($+0.51$ *e*) indicates that electrons are transferred just from this atom to the C_{60} core, which manifests the acceptor properties in the $(\eta^2\text{-C}_{60})\text{Pd}[\text{P}(\text{Ph}_2)\text{C}_5\text{H}_4]_2\text{Fe}$ complex.

References

1. A. Hirsch, *The Chemistry of Fullerenes*, Georg Thieme, Stuttgart, 1993, 204 pp.

2. I. V. Stankevich and V. I. Sokolov, *Izv. Akad. Nauk, Ser. Khim.*, 2004, 1749 [*Russ. Chem. Bull., Int. Ed.*, 2004, **53**, 1824].
3. P. J. Fagan, J. C. Calabrese, and B. Malone, *Science*, 1991, **252**, 1160.
4. A. L. Balch and M. M. Olmstead, *Chem. Rev.*, 1998, **98**, 2123.
5. E. Sulman, V. Matveeva, N. Semagina, I. Yanov, V. Bashilov, and V. Sokolov, *J. Mol. Catal. A: Chem.*, 1999, **146**, 257.
6. H. Kunkely and A. Vogler, *Inorg. Chim. Acta*, 1996, **250**, 375.
7. V. V. Bashilov, T. V. Magdesieva, D. N. Kravchuk, P. V. Petrovskii, A. G. Ginzburg, K. P. Butin, and V. I. Sokolov, *J. Organomet. Chem.*, 2000, **599**, 37.
8. D. S. Urch, in *Electron Spectroscopy — Theory, Techniques and Application*, Vol. 3, Eds G. R. Brundle and A. D. Baker, Academic Press, London, 1979, 1.
9. A. V. Okotrub and L. G. Bulusheva, *Fuller. Sci. Technol.*, 1998, **6**, 405.
10. A. D. Becke, *J. Chem. Phys.*, 1993, **98**, 5648.
11. *Jaguar 3.5*, Schrodinger, Inc., Portland (OR), 1998.
12. L. G. Bulusheva, A. V. Okotrub, A. V. Gusel'nikov, V. D. Yumatov, V. V. Bashilov, and V. I. Sokolov, *J. Mol. Struct.*, 2005, **749**, 199.
13. V. V. Bashilov, P. V. Petrovskii, V. I. Sokolov, S. V. Lindeman, I. A. Guzey, and Yu. T. Struchkov, *Organometallics*, 1993, **12**, 991.
14. D. P. Chong, O. V. Gritsenko, and E. J. Baerends, *J. Chem. Phys.*, 2002, **116**, 1760.
15. G. Schaftenaar and J. H. Noordik, *J. Comput.-Aided Mol. Design*, 2000, **14**, 123.
16. J.-H. Guo, Y. Luo, O. Vahtras, P. Skytt, N. Wassdahl, H. Ågren, and J. Nordgren, *Chem. Phys. Lett.*, 1994, **227**, 98.
17. L. G. Bulusheva and A. V. Okotrub, *Rev. Inorg. Chem.*, 1999, **19**, 79.
18. J. W. Rabalais, L. O. Werme, T. Bergmark, L. Karlsson, M. Hussain, and K. Siegbahn, *J. Chem. Phys.*, 1972, **57**, 1185.
19. A. P. Sadovskii and E. A. Kravtsova, *Koord. Khim.*, 1978, **4**, 418 [*Sov. J. Coord. Chem.*, 1978, **4** (Engl. Transl.)].

Received December 20, 2004